

# Development of imaging arrays for solar UV observations based on wide band gap materials

Udo Schühle<sup>\*a</sup>, Jean-François Hochedez<sup>b</sup>, José Luis Pau, Carlos Rivera, Elias Muñoz<sup>c</sup>, José Alvarez, Jean-Paul Kleider<sup>d</sup>, Philippe Lemaire<sup>e</sup>, Thierry Appourchaux, Bernhard Fleck, Anthony Peacock<sup>f</sup>, Mathias Richter, Udo Kroth, Alexander Gottwald<sup>g</sup>, Marie-Claude Castex<sup>i</sup>, Alain Deneuve, Pierre Muret<sup>k</sup>, Milos Nesladek<sup>m</sup>, Franck Omnes<sup>n</sup>, Joachim John, Chris Van Hoof<sup>p</sup>

<sup>a</sup>Max-Planck-Institut für Aeronomie; <sup>b</sup>Royal Observatory of Belgium; <sup>c</sup>Universidad Politécnica de Madrid, <sup>d</sup>Laboratoire de Génie Electrique de Paris, <sup>e</sup>Institut d'Astrophysique Spatiale Orsay, <sup>f</sup>European Space Agency Noordwijk, <sup>g</sup>Physikalisch-Technische Bundesanstalt Berlin, <sup>i</sup>Université de Paris-Nord, <sup>k</sup>Laboratoire d'Etudes des Propriétés Electroniques des Solides CNRS Grenoble, <sup>m</sup>IMO Institute for Material Research Diepenbeek, <sup>n</sup>Centre de Recherche sur l'Hétéro-Epitaxie et ses Applications (CRHEA-CNRS) Valbonne, <sup>p</sup>Interuniversity Microelectronics Ctr. Leuven

## ABSTRACT

Solar ultraviolet imaging instruments in space pose most demanding requirements on their detectors in terms of dynamic range, low noise, high speed, and high resolution. Yet UV detectors used on missions presently in space have major drawbacks limiting their performance and stability. In view of future solar space missions we have started the development of new imaging array devices based on wide band gap materials (WBG), for which the expected benefits of the new sensors - primarily visible blindness and radiation hardness - will be highly valuable. Within this initiative, called "Blind to Optical Light Detectors (BOLD)", we have investigated devices made of AlGa-nitrides and diamond. We present results of the responsivity measurements extending from the visible down to extreme UV wavelengths. We discuss the possible benefits of these new devices and point out ways to build new imaging arrays for future space missions.

**Keywords:** Detector, imager, devices, wide bandgap, ultraviolet, AlGa<sub>N</sub>, Ga<sub>N</sub>, diamond, Sun

## 1. INTRODUCTION

The solar atmosphere is highly structured and dynamic on all spatial scales that are currently possible to observe from Earth and from space. Recent solar space missions have revealed major breakthroughs in the understanding of the structural and dynamic processes taking place on the Sun. The progress was made possible in great deal by high resolution remote sensing instrumentation<sup>1</sup>. With the large temperature range of the different layers of the Sun's atmosphere, emitting in the far ultraviolet down to extreme ultraviolet wavelengths, it was possible to observe each atmospheric regime within its finite bandwidth of emission by selecting instrumentation with high spectral resolution. However, the observations of fine structures in the solar photosphere, chromosphere, transition region, and the corona still suffer from limited spatial resolution achieved by instruments flown up to now. Current solar atmospheric studies show that improved ultraviolet observations would be of paramount value to future advances in the field. This requires focal plane instrumentation with imaging arrays of large number of image elements (pixels).

As it was always the case, future observations from space will benefit from miniaturization and mass reduction of instrumentation. For optical telescopes the instruments can be made smaller by reducing the focal length, but this comes with a reduction of the image scale. Thus, smaller image elements must be used to keep the same resolution element per pixel. It is thus a goal to develop imaging arrays with large number but smallest size of pixels.

Despite the fact that the brightness of the Sun is generally very high, the signal collected by an image element in the ultraviolet is usually very weak for several reasons: First, instrument sensitivities are low, because of low efficiency of

optical components (mirrors and filters), secondly, because the observations are mainly required to be monochromatic – preferentially in one single spectral line –, and the radiance of the emitting atmospheric element is not high in the ultraviolet.

Fortunately, degradation of solar space optical instruments by contamination has been largely overcome by well understood cleanliness strategies<sup>2</sup>. However, the imaging devices in the focal planes of instruments have been the limiting factors of the stability of responsivity in recent solar missions<sup>3,4</sup>. From this experience the demand is driven for new detector devices that are more stable in the space environment<sup>5,6</sup>. Wide bandgap materials (WBGm) have shown to be very promising candidates for UV imaging devices. Particularly, diamond<sup>6</sup> and aluminium gallium nitrides (AlGaN)<sup>7</sup> have been well characterized recently.

Here we present some examples of new devices that have been built, based on wide band gap materials and show first performance results.

## 2. PRESENT AND FUTURE DETECTOR DESIGN CONCEPTS

### 2.1 Present UV detectors and their shortcomings

The wavelength region of solar atmospheric emission ranges from the near ultraviolet to the extreme UV. The present focal plane detectors for this wavelength range are based on either back-side thinned CCDs or on microchannel plate intensifiers with a position encoding and digitization device, which can be a special anode array with digitization electronics or an optical transfer to a CCD. Both technologies exhibit shortcomings that are severely limiting their performance. These have been detailed in a previous publication by Hochedez et al.<sup>8</sup>. We summarize here the major points, because they set the design requirements for new detectors:

Detectors based on CCDs suffer from several drawbacks related to the silicon-based technology:

- CCDs are based on silicon which is most sensitive in the visible and much less in the UV. One thus has to introduce filters to make them “solar blind”, which attenuates by many orders of magnitude the largest portion of the solar radiation but also the solar UV to be detected.
- CCDs have high dark current. To reduce the dark signal, CCDs must be operated at low temperatures. This is technically challenging and costly in space missions. The cold detector surface makes it a cold trap for any condensable contaminant inside the instrument, leading to very unstable performance due to contaminant build-up on the sensitive surface.
- CCDs are not “radiation hard”. The ionizing radiation of the space environment leads to “cosmic-ray hits” (points and streaks) puzzling the images. In addition, the radiation results in damage to the charge collection efficiency (CCE) of the affected channel, resulting in a non-uniform spatial response of the array.
- CCDs are insensitive in the VUV. In the vacuum-ultraviolet (VUV) range the penetration depth of photons in silicon is particularly low, and the sensitivity is reduced. One solution to this problem is image intensifiers based on microchannel plates (MCPs). They are inherently solar blind and VUV sensitive (with special photocathode coating), but they have other drawbacks as follows.
- Image intensifiers need pixel sensors for position encoding, which may be CCDs, incorporating thereby some of the previous problems, or anode arrays that sense the position of the incident photon by centroiding the electron cloud produced by the channel plate, and converting it into a pixel array. The latter avoids the drawbacks of CCDs, is inherently less sensitive to cosmic rays, and needs no cooling. But microchannel plates have major additional drawbacks.
- MCPs need high voltage for amplification.
- MCPs have limited resolution due to the pore size of the channels.

- MCPs have limited dynamic range due to gain saturation at high counts rates.
- MCPs lead to distortion of the image due to the imperfect image transfer between the photocathode and the anode by the residual alignment errors between the channels and the gap between the MCP and the anode (or the CCD).
- The response of MCPs is unstable due to scrubbing, i. e., their gain reduces continuously during usage. This makes the calibration difficult to maintain. The high voltage must be increased to compensate for scrubbing.

The large number of shortcomings limit the performance of the sensors or at least increase the technical challenges to overcome these limitations. New detector devices based on wide bandgap materials (WBG) - diamond or aluminum-gallium-nitrides - are known candidates that can overcome many of the restrictions listed above.<sup>5,6,7</sup>

The wide bandgap materials produce such low dark current that allows the sensing elements to operate at ambient or even higher temperatures. This avoids the need for cooling and bake-out hardware and the contamination risk related to it. Materials can be selected with such large bandgaps that they are insensitive to the most intense part of the solar spectrum, which makes the detectors “solar-blind”. Their compact crystal structure provides better radiation hardness, because the smaller atomic weight of the materials provides a smaller cross-section to ionizing radiation and fewer damaging artifacts due to cosmic ray hits. The WBG have a higher electrical breakdown resistance. Thus the field strength for charge collection can be higher. As a result the pixel size can potentially be much smaller than in silicon. The WBG are sensitive to the VUV, which avoids entirely all the drawbacks related to microchannel plate intensifiers. No oxide layer is needed on the sensitive substrate surface. This will improve the quantum efficiency, its uniformity of response, and its stability compared to silicon-based sensors. The WBG have an exceptional chemical stability and are very hard. It can thus be expected that such devices can face extreme working conditions, like it is necessary for UV detectors in solar space applications: intrinsic EUV/VUV sensitivity and stability under high irradiation, hardness against cosmic rays, high temperature operation, and stability against chemical degradation.

## 2.2 New Detector design concepts

Generally, basic semiconductor sensor devices can be classified in four classes<sup>9,10</sup>: photoconductive devices, p-n and p-i-n junction photodiodes, Schottky barrier diodes, and metal-semiconductor-metal photodiodes. All types of these structures have been successfully developed and devices are being investigated. Diamond and aluminum-gallium-nitride materials are currently under investigation. Due to the low penetration depth of UV photons in these materials, mostly co-planar structures are being fabricated and investigated, although bulk diamond devices may be attractive as wide-band detectors<sup>11</sup>.

It is anticipated that taking advantage of well established silicon-based read-out circuitry is the best approach to arrive at the completion of an imaging device with high versatility. This will result in hybrid sensors that will implement their sensing function from nitride or diamond, and their image read-out function through a CMOS active pixel circuitry (APS). The APS scheme provides high flexibility regarding on-chip logic and image processing, which might be required by special applications (e.g., on-chip binning, arithmetics for polarimetry). Hybridization using flip-chip integration with indium bump bonding currently is possible down to a resolution of  $\sim 10 \mu\text{m}$  pitch (px to px distance), presently limiting miniaturization. It requires a free standing, very thin membrane of the sensing material to be bonded to a read-out circuit (ROIC), whereas a direct bonding (through the wafer) may also be possible.

### 2.2.1 Diamond devices

Diamond is a well-known material for the detection of radiation of energy above the 5.5 eV bandgap energy. Besides its favorable mechanical, thermal, and optical properties, diamond exhibits high carrier mobility and high resistance to electrical breakdown<sup>12</sup>. Both, polycrystalline and monocrystalline devices are being fabricated with excellent electrical performance characteristics. Presently, residual defects and impurities of the CVD diamond layers are limiting the VUV efficiency and solar blindness performance.

Control of the geometry and dimensions of the active diamond layers is also a challenge. Progress has been made by using reactive ion etching (RIE). This technique opens the possibility of defining an array of lines and columns which delineates a pixel at each intersection. For diamond, RIE can be achieved with an oxygen plasma which acts owing to both ionic bombardment (anisotropic process) and chemical etching by oxygen radicals. A metallic mask must be first deposited; then a pattern is drawn by lithography and etched in order to protect the diamond layer where it must remain. The concentration of the active species in the plasma and ionic bombardment can be adjusted independently when Electron Cyclotron Resonance (ECR) plasma are used. One problem comes from the re-deposition of mask particles which may be sputtered from the mask by ionic bombardment. It leads to whiskers which remain at the bottom of the etched zone as one can see in the scanning electron microscope picture of Figure 1-a. However, this problem can be avoided by choosing an appropriate material for the metallic mask and proper bias voltages. This is done here and illustrated in Figure 1-b. In both cases, the microwave power density is  $1 \text{ W/cm}^2$  at 2.45 GHz, with 3 mbar of  $\text{O}_2$ , but the metallic mask is made of Al and the bias voltage is adjusted up to  $-150 \text{ V}$  in case a, whereas Ti is used in case b with a bias voltage of  $-30 \text{ V}$ . This is the demonstration that a clean and flat bottom can be obtained in the etched zones. Such a technique opens the route for diamond devices with a complex architecture.

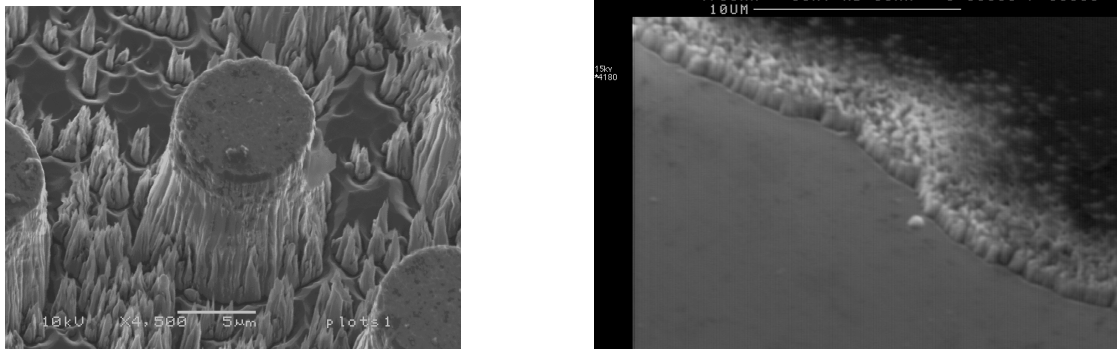


**Figure 1-a and 1-b:** Scanning electron microscope image of the surface produced by reactive ion etching using an electron cyclotron resonance source. In the first case (left) an aluminium mask was used and in the second case (right) a titanium mask was used (see text for details).

### 2.2.2 AlGa<sub>x</sub>N devices

Due to their direct bandgap, AlGa<sub>x</sub>N photodetectors present abrupt responsivity cut-offs that, thanks to the possibility to vary the bandgap from 3.4 eV to 6.2 eV, makes them very adequate for the fabrication of visible- and solar-blind devices. The lack of lattice matched substrates has forced to use foreign substrates for III-nitride growth, with the consequent difficulties to improve the material quality. However, the recent continuous advances in the growth techniques have led to the successful development of AlGa<sub>x</sub>N photodetectors with different device structures.

Al<sub>x</sub>Ga<sub>1-x</sub>N ( $0 < x < 0.60$ ) layers were grown by metal-organic chemical vapor deposition (MOCVD) and radio frequency plasma assisted molecular beam epitaxy (rf-PAMBE) on sapphire and silicon substrates, respectively. The surface roughness of the samples presented RMS values lower than 3 nm in  $10 \times 10 \mu\text{m}^2$  areas. Our efforts to improve the device structure and reduce the pixel devices have been mainly conducted in two kinds of devices: metal-semiconductor-metal (MSM) and Schottky photodiodes. Different metals and geometries were tried in order to get better device characteristics. The fabrication of the MSMs was based in the deposition of interdigitated contacts, which fit adequately the device characteristics. It was found that the responsivity of the devices strongly depends on the metal contact, the finger widths and pitches, and the applied bias. We have used a metallic contact consisting of a Pt (400 Å)/Ti (50 Å)/Au (1000 Å) tri-layer, and finger widths and pitches ranged from  $2 \mu\text{m}$  to  $7 \mu\text{m}$ . In contrast to MSMs, Schottky photodiodes can be operated at zero bias voltage, avoiding non-desirable contributions to the signal from the photoconductive gain, which enhance the dark current and the  $1/f$  low-frequency noise. The semitransparent Au layer

deposition becomes very critical in this structure and its optical characterization is very important for the assessment of the device performance.

As an example, Figure 2 shows two samples of MSM and Schottky photodiodes recently fabricated and tested at the single-pixel level. The details of their fabrication have been published by Muñoz, et al.<sup>13</sup>. Preliminary 1x6 AlGaIn-based photodetector arrays have also been manufactured with pixel active areas as low as  $30 \times 30 \mu\text{m}^2$ , and finger widths and pitches of  $2 \mu\text{m}$  (Figure 3-a). These micro-arrays allow us to study the homogeneity of the samples, the pixel-to-pixel cross-talk or the image persistence.

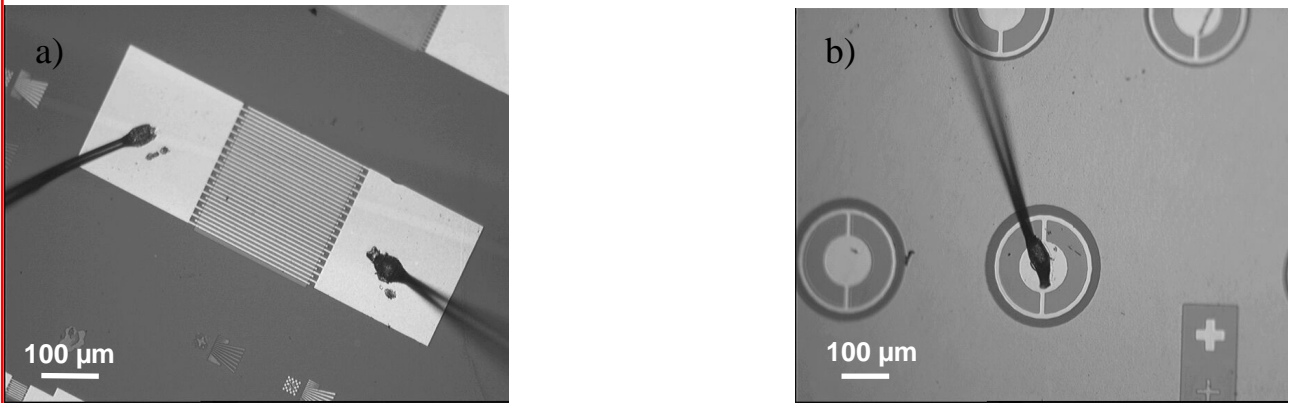


**Figure 2.** a) MSM and b) Schottky barrier single-photodiodes fabricated for their test under synchrotron radiation.

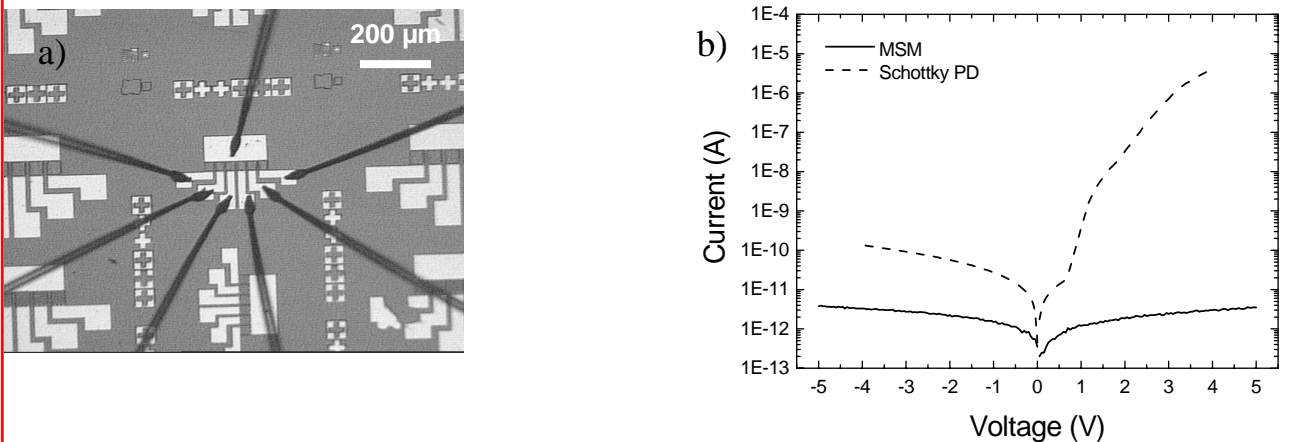


**Figure 3.** a) 1x 6 linear micro-array of MSM photodiodes fabricated on AlGaIn/Si(111) samples. b) Typical I-V characteristic curves of MSM and Schottky photodiodes.

Typical I-V characteristics of MSM and Schottky photodiodes are shown in the Figure 3-b). MSMs present very small dark current values ( $< 10 \text{ pA}$  at  $\pm 5 \text{ V}$ ), according to transport behavior predicted by the thermoionic emission theory at reverse biases through a metal-semiconductor junction. On the other hand, the diode characteristic of the Schottky

barrier photodetectors yields a current level four orders of magnitude higher at a forward bias of 4 V than at  $-4$  V. This electrical performance reveals a good quality of the ohmic and Schottky contacts deposited on the sample surface.

### 2.3 Past and future measurement campaigns

Several measurement campaigns have already provided results, briefly reported in this section. The tests extend from the EUV to the visible, covering the range of anticipated benefits. The manufactured devices are being characterized with synchrotron beam lines, laser sources and monochromated UV lamps in several European facilities. The main focus has been on assessing the detector UV efficiency, solar-blindness (visible light rejection), radiation-hardness, and ageing robustness, in addition to testing their fundamental, electrical functions.

The spectral response of the AlGaIn photodetectors in the NUV was carried out at University of Madrid by using a 150 W Xe arc lamp coupled to a Jobin-Yvon H-25 monochromator. The responsivity values at 257 nm were obtained by exciting with a second harmonic generator pumped by the 514-nm-line of an Ar<sup>+</sup> laser.

Photoconductivity of diamond films has been measured at different wavelengths using VUV lasers at 193 nm and 266 nm at the LPL of University of Paris<sup>11</sup>. By choice of the laser wavelength the above band gap and sub-gap properties may be studied, and the high laser intensity allows the measurements of photoresponse as a function of laser fluence by way of a beam attenuator.

The measurements of responsivity in EUV and VUV spectral ranges have been carried out by the Physikalisch-Technische Bundesanstalt (PTB) in Germany at the electron storage ring BESSY II. The spectral range between 40 nm and 250 nm was covered by the monochromatized synchrotron radiation from a bending magnet of the BESSY electron storage ring. This so-called Normal-incidence beamline for detector calibrations in the PTB radiometry laboratory allows us to measure absolute responsivity of devices by comparison with a calibrated PtSi-Schottky photodiode<sup>14</sup>. In such a large spectral range, out-of-band radiation must be avoided by suppressing higher order light from the monochromator using filters with different long-pass characteristics: below 140 nm a Ar gas cell is introduced in the beamline, above 120 nm a MgF<sub>2</sub> filter is used. For the very small devices a rastering of the beam with the sample is necessary, which is accomplished by linear drives and control with automatic scanning procedures.

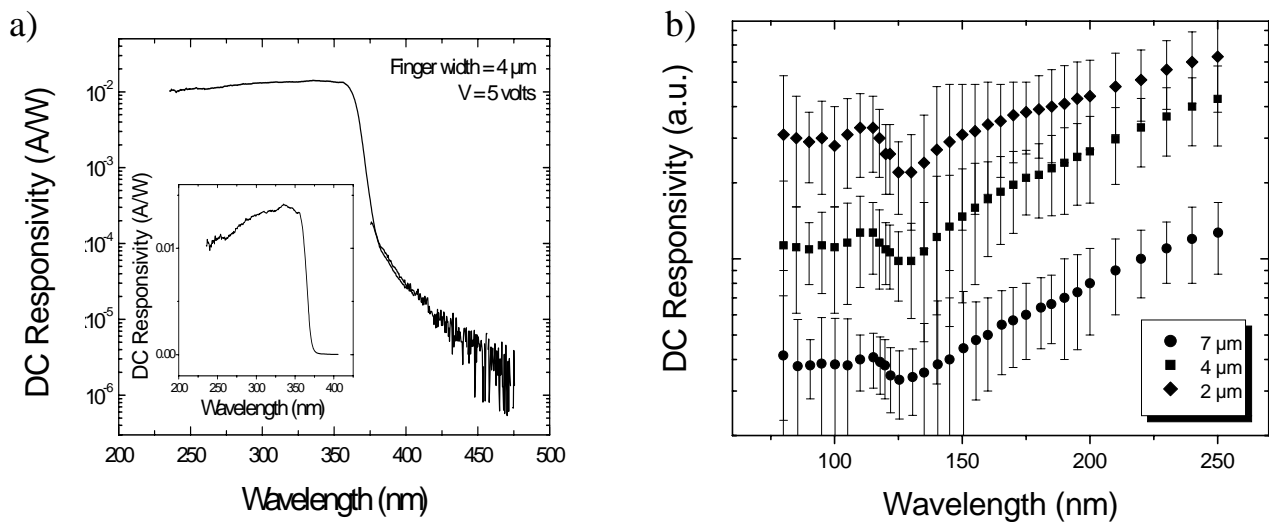


**Figure 4.** Visible and UV responsivity of GaN MSM structure (a) and spectral responsivities (b) in the VUV of three MSM devices with finger widths and spacings between 2 μm and 7 μm.

## 2.4 Responsivity from the EUV to the NUV

Two promising results are presented in Figure 4. The UV-VIS measurements (shown in Figure 4-a) achieved visible-to-UV rejection rates that exceed four orders of magnitude, but we anticipate still higher rates in the future due to thinning techniques and improvement of the crystal quality. For energies above the bandgap, it shows a quite flat response which enables the MSM photodiodes to detect radiation energies in the VUV.

Figure 4-b shows the spectral response of three GaN MSM photodiodes with 2, 4, and 7  $\mu\text{m}$ -wide electrodes and active areas of  $500 \times 500 \mu\text{m}^2$ . The thinner the electrode is, the higher is the responsivity, thanks to the major number of electrodes included inside the detector active area which reduces the dead areas of the device.

Recently, the absolute spectral responsivity could be measured over a wide wavelength range in the EUV and VUV. The GaN Schottky diode structures show a very good response throughout the whole range from 40 nm to 250 nm (see Figure 5). The results show that the photoresponse diminishes with the wavelength in the 250 – 130 nm range. As the absorption coefficient increases in the same range, the responsivity decreases as the light absorption increases. Therefore, the origin of this reduction seems to be related to surface characteristics involving oxide formation or high surface recombination rates. For wavelengths lower than 130 nm, the photoresponse even increases rapidly with the photon energy, while below 80 nm the response shows a linear declining slope which is corresponding to a constant quantum efficiency over this range. Two phenomena must be taken in account in this case. On one side, there is a change in the absorption coefficient behavior since it begins to decrease with the photon energy. On the other side, the photon energy is higher than the ionization energy (the average amount of energy given up by the incident radiation in the process of generating a single electron-hole pair), which can cause the creation of multiple electron-hole pairs by an incident photon. These processes have to be carefully studied in the future to optimize the spectral response in this photon energy regime.

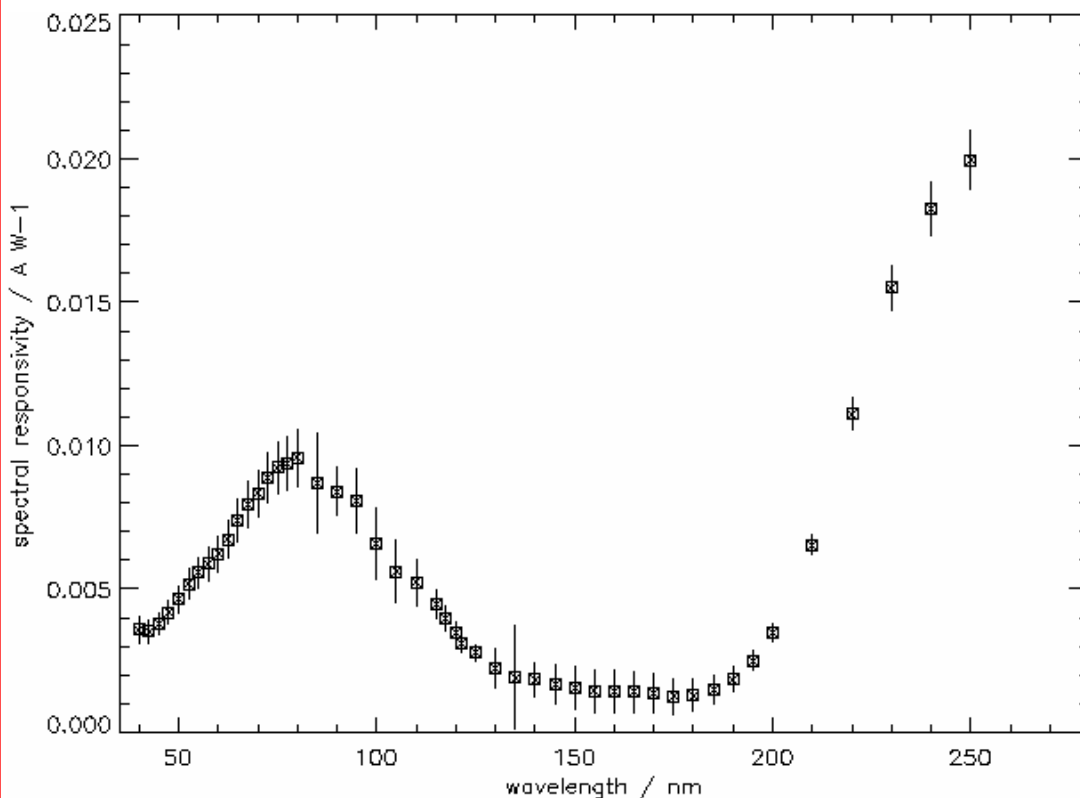


**Figure 5.** Absolute spectral response (in A/W) of a GaN Schottky diode structure in the EUV and VUV.

### 3. CONCLUSIONS AND OUTLOOK

The techniques are established to produce sensitive devices of wide bandgap materials, and first steps have been made towards imaging devices by fabricating small arrays. We expect in the near future, innovative detectors that will give a new leap to UV imaging. It will benefit the astrophysical observations but also many other applications like, e.g., x-ray imaging in medicine or 13-nm lithography, Earth and environmental remote sensing, flame and combustion diagnostics, to name just a few.

An early flight demonstration of solar observations with the new devices is sought for, and this will be accomplished within the *Proba-2* mission of ESA. Proba (Project for on-board autonomy) is conceived for the purpose of demonstrating new on-board technologies and opportunities and benefits of on-board autonomy. The *LYRA instrument* (Lyman-alpha Radiometer) is a small, compact instrument that is currently under development for the Proba-2 mission. It will monitor the solar irradiance at four spectral channels in the ultraviolet, taking advantage of the wide band gap materials as their sensing devices. Although the four channels are using non-imaging sensors, their application will demonstrate their superiority in terms of VUV sensitivity, solar blindness, calibration stability, and radiation hardness. The LYRA instrument will demonstrate usefulness of the concept, crucial for future space solar missions.

### REFERENCES

1. Fleck, B., Marsch, E., Schwenn, R., Antonucci, E., Bochsler, P., Bougeret, J.-L., Harrison, R. A., Marsden, R., Vial, J.-C., "Solar Orbiter – A high-resolution mission to the Sun and inner heliosphere", in *proceedings of AAS/Solar Physics Division Meeting*, 32, 0296, 2000.
2. Schühle, U., "Cleanliness and Calibration Stability of UV Instruments on SOHO", in *Innovative Telescopes and Instrumentation for Solar Astrophysics*, S. L. Keil, S. V. Avakyan (Eds.), *Proc. SPIE*, 4853, 88 - 97, 2003.
3. Schühle, U., Thomas, R., Hochedez, J.-F., "The Solar Orbiter Mission and Design Recommendations", in *The Radiometric Calibration of SOHO*, ISSI Scientific Report SR-002, 361 - 370, ESA Publ. Div., Noordwijk, 2002.
4. Thompson, W. T., "UV detectors aboard SOHO", *Proc. SPIE*, 3764, 196 - 208, 1999.
5. Hochedez, J.-F., Lemaire, P., Pace, E., Schühle, U., and Verwichte, E., "Wide bandgap EUV and VUV imagers for the Solar Orbiter", ESA SP-493, 245 - 250, 2001.
6. Hochedez, J.-F., Bergonzo, P., Castex, M.-C., Dhez, P., Hainaut, O., Sacchi, M., Alvarez, J., Boyer, H., Deneuille, A., Gibart, P., Guizard, B., Kleider, J.-P., Lemaire, P., Mer, C., Monroy, E., Muñoz, E., Muret, P., Omnes, F., Pau, J.L., Ralchenko, V., Tromson, D., Verwichte, E., and Vial, J.-C., "Diamond UV detectors for future solar physics missions", *Diamond and Related Materials* 10/3-7, 669 - 676, 2001.
7. Sandvik, P., Mi, K., Shahedipur, F., McClintock, R., Yasan, A., Kung, P., Razeghi, M., "Al<sub>x</sub>Ga<sub>1-x</sub>N for solar-blind UV detectors", *J. Cryst. Growth* 231, 366 - 370, 2001.
8. Hochedez, J.-F., Schühle, U., Pau, J.L., Alvarez, J., Hainaut, O., Appourchaux, T., Auret, D., Belky, A., Bergonzo, P., Castex, M.C., Deneuille, A., Dhez, P., Fleck, B., Haenen, K., Idir, M., Kleider, J.P., Lefevre, E., Lemaire, P., Monroy, E., Muret, P., Munoz, E., Nesladek, M., Omnes, F., Pace, E., Peacock, A., Van Hoof, C., "New UV detectors for solar observations", in *Innovative Telescopes and Instrumentation for Solar Astrophysics*, S. L. Keil, S. V. Avakyan (Eds.), *Proc. SPIE*, 4853, 88 - 97, 2003.
9. Razeghi, M., Rogalski, A., "Semiconductor ultraviolet detectors", *J. Appl. Phys.* 79, 7433, 1996.
10. Carrano, J. C., Li, T., Eiting, C. T., Dupuis, R. D., Campbell, J. C., "Comprehensive characterization of metal-semiconductor-metal ultraviolet photodetectors fabricated on single-crystal GaN", *J. Appl. Phys.* 83, 6148, 1998
11. Lefevre, E., Achard, J., Castex, M.C., Schneider, H., Beuillé, C., Tardieu, A., "Bulk photoconductivity of CVD diamond films for UV and XUV", *Diamond and Related Materials*, 12, 642, 2003.
12. Pan, L.S., Kania, D.R., (Eds.), "Diamond: Electronic Properties and Applications", Kluwer, Boston, 1995.
13. Muñoz, E., Monroy, E., Pau, J. L., Calle, F., Omnès, F., Gibart, P., "III-nitrides and UV detection", *J. Phys.: Condens. Matter* 13, 7115, 2001.
14. Richter, M., Hollandt, J., Kroth, U., Paustian, W., Rabus, H., Thornagel, R., Ulm, G., "Source and detector calibration in the UV and VUV at BESSY II", *Metrologia* 40, 107 - 110, 2003.